Dimerization of MoMuLV Genomic RNA: Redefinition of the Role of the Palindromic Stem−Loop H1 (278−303) and New Roles for Stem−Loops H2 (310−352) and H3 (355−374)

Marc De Tapia, Vincent Metzler,‡ Marylène Mougel,§ Bernard Ehresmann, and Chantal Ehresmann*

Unité Propre de Recherche 9002 du CNRS, Institut de Biologie Moléculaire et Cellulaire, 15 rue René Descartes, 67084 Strasbourg Cedex, France

Received January 6, 1998; Revised Manuscript Received February 24, 1998

ABSTRACT: Genomic RNAs from retroviruses are packaged as dimers of two identical RNA molecules. In Moloney murine leukemia virus, a stem−loop structure (H1) located in the encapsidation domain Ψ (nucleotides 215−564) was postulated to trigger RNA dimerization through base pairing between auto complementary sequences. The Ψ domain also contains two other stem−loop structures (H2 and H3) that are essential for RNA packaging. Since it was suspected than H1 is not the only element involved in RNA dimerization, we systematically investigated the dimerization capacity of several subdomains of the first 725 nucleotides of genomic RNA. The efficiency of dimerization of the various RNAs was estimated by measuring their apparent dissociation constants, and the specificity was tested by competition experiments. Our results indicate that the specificity of dimerization of RNA nucleotides 1−725 is driven by motifs H1−H3 in domain Ψ. To define the relative contributions of these elements, RNA deletion mutants containing different combinations of H1−H3 were constructed and further analyzed in competition and kinetic experiments. Our results confirm the importance of H1 in triggering dimerization and shed new light on the mechanism of dimerization. H1 is required to provide a stable dimer, probably through the formation of extended intermolecular interactions. However, H1-mediated association is a slow process that is kinetically enhanced by H3, and to a lesser extent by H2. We suggest that they facilitate the recognition between the two RNAs, most likely through their conserved GACG loops. Our results reinforce the idea that dimerization and packaging are two closely related processes.

Retroviruses display the unique property of packaging two identical copies of (+) strand RNA. They are physically linked near their 5′ end at the dimer linkage structure (DLS)[1] in an apparent parallel orientation (*1*, *2*; for review, see ref *3*). One major consequence of the dimeric nature is recombination between the two RNA molecules. Recombination is thought to be essential for the virus to repair damage in its genome, to increase genetic diversity, and to escape host immune response and antiviral therapy (*4*−*8*). On the other hand, dimerization of genomic RNA has been postulated to be linked to encapsidation, as sequences involved in the dimerization of several retroviral RNAs have been mapped to regions overlapping identified encapsidation signals (*9*−*14*). The involvement of a dimerization element in packaging HIV-1 RNA was recently confirmed (*15*−*18*). Moreover, the retroviral nucleocapsid protein (NCp), which is required for encapsidation, was shown to enhance dimerization (*10*, *11*, *19*). Thus, it appears that the dimerization process represents a key step in the viral life cycle. In line with this view, the deletion of a stem−loop structure, called the DIS, which is required for initiating HIV-1 RNA dimerization, was shown to severely reduce infectivity due to defects in both packaging and proviral DNA synthesis (*17*).

The discovery of spontaneous dimerization of in vitro generated RNAs induced by cations has permitted some insight into the dimerization mechanism (reviewed in refs *14* and *18*). For MoMuLV, the DLS was previously mapped by deletion analysis in the leader sequence between the major splice donor site and the *gag* start codon (nucleotides 215−564) (*11*). This region overlaps the minimal encapsidation Ψ domain (nucleotides 215−374) (*20*−*22*). In a previous study, we showed with chemical probing experiments that the Ψ region can form an independent and highly structured domain (*23*) (Figure 1). Dimerization was found to induce base reactivity changes in restricted and defined areas in Ψ (*23*), and also in both upstream and downstream regions (*24*). These reactivity changes could be interpreted to be the result of intermolecular interactions and/or intramolecular rearrangements. Our data pointed to a putative dimerization element in Ψ, corresponding to a conserved stem−loop structure (nucleotides 278−303, named H1) containing an

* To whom correspondence should be addressed. Fax: 33-3 88 60 22 18. E-mail: ehresmc@ibmc.u-strasbg.fr.

‡ Present address: Zoologisches Institut der Universität Bern, Abteilung für Entwicklungsbiologie, Baltzerstrasse 4, 3012 Bern, Switzerland.

§ Present address: Unité Mixte de Recherche CNRS, Institut de Génétique Moléculaire de Montpellier, 1919 route de Mende, 34033 Montpellier, France.

[1] Abbreviations: DIS, dimerization initiation site; DLS, dimer linkage structure; HaSV, Harvey sarcoma virus; HIV, human immunodeficiency virus; MoMuLV, Moloney murine leukemia virus; NCp, nucleocapsid protein; SD, splice donor; ASLV, avian sarcoma leukosis virus; SIV, simian immunodeficiency virus; SNV, spleen necrosis virus.

S0006-2960(98)00030-0 CCC: $15.00
Published on Web 04/11/1998

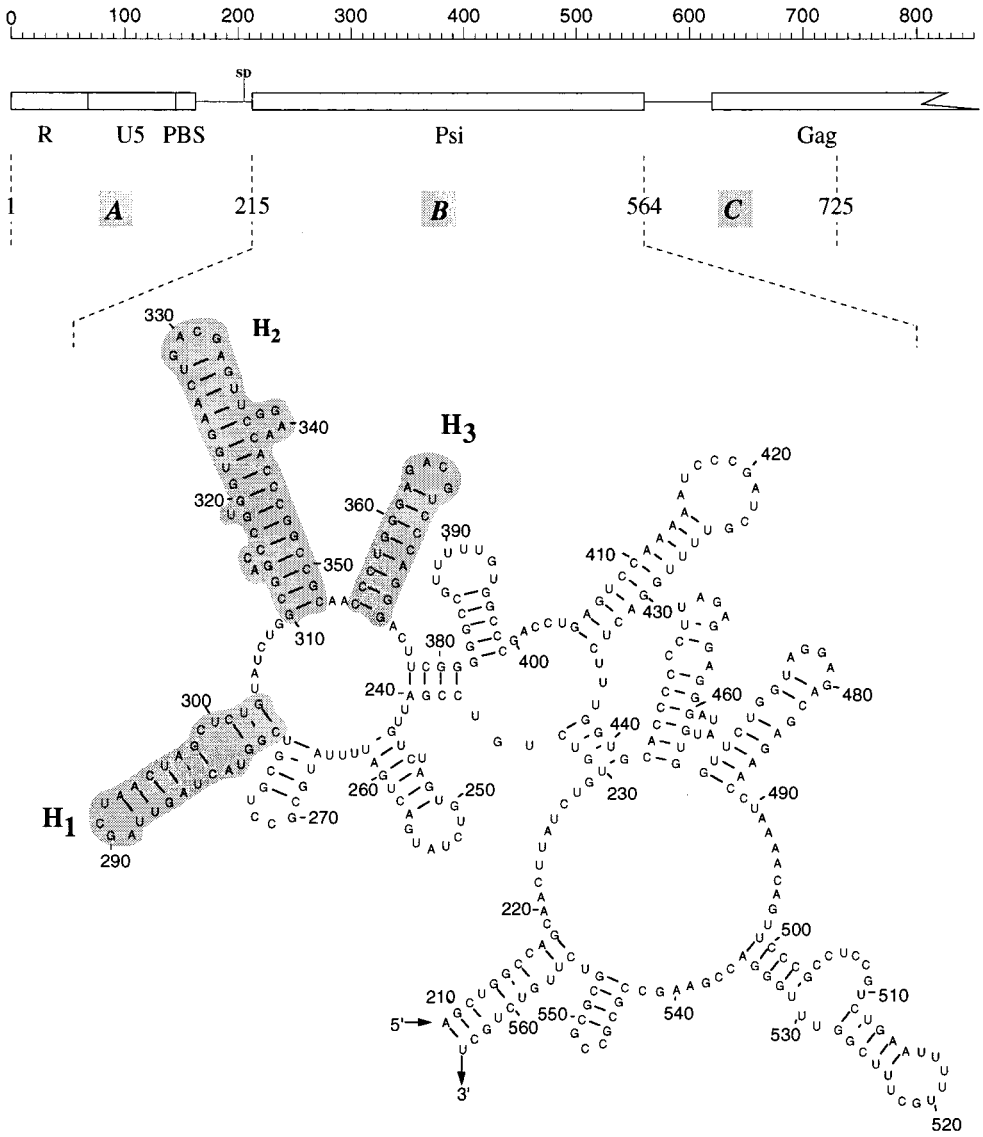

FIGURE 1: Schematic organization of the 5′ region of MoMuLV and secondary structure of the Ψ domain. The different functional elements are indicated: R, redundant sequence; U5, unique 5′ sequence; PBS, primer binding site; and SD, splice donor site. The three stem−loop structures (H1−H3) are shaded. The secondary structure model is from Tounekti et al. (*23*).

autocomplementary sequence (nucleotides 283−298). The involvement of H1 was confirmed by antisense oligodeoxyribonucleotide inhibition experiments and thermodynamic studies on the isolated Ψ region and derived fragments (*25*). The proposed dimerization mechanism involved loop−loop recognition followed by extension of intermolecular annealing. The transition toward the extended duplex has been proposed to be promoted by NCp10 (*26*). The proposed mode of loop−loop recognition is reminiscent of the HIV-1 dimerization process (*27*−*34*). However, despite the existence of similarities in the dimerization mechanism of retroviral RNAs, some particulars are observed. Indeed, downstream sequences are involved in further stabilization of the HIV-1_{Mal} RNA dimer (*30*, *35*) but not in HIV-1_{Lai} (*36*, *37*). In Harvey sarcoma virus, a virus closely related to MoMuLV, it was shown that multiple regions of RNA were able to promote dimerization (*38*). In the case of MoMuLV, the postulated DLS also contains two other stem−loop structures, named H2 and H3 (Figure 1), adjacent to H1, which have been shown to be required for efficient encapsidation in MoMuLV (*16*, *22*) and spleen necrosis virus (*39*). Both hairpins are highly conserved among murine type C retroviruses and contain a GACG tetraloop.

In this work, we investigated the dimerization capacity of several domains of the 1−725 region of MoMuLV RNA and the relative contributions of the three stem−loop elements (H1−H3) in the 215−564 Ψ domain. The dimerization efficiency of the various truncated or mutant RNAs was estimated by measuring their apparent dissociation constants (K_d). The specificity of dimerization was further tested by competition experiments. Our results demonstrate the involvement, in addition to the H1 element previously described, of the two other structural elements, H2 and H3. By measuring the association and dissociation kinetics of dimerization of deletion RNA mutants, we could define the relative contributions of the three stem−loop elements in the dimerization process.

EXPERIMENTAL PROCEDURES

Plasmid Construction and RNA Synthesis. Standard procedures were used for restriction enzyme digestion and plasmid construction (*40*). *Escherichia coli* JM109 cells

were used for plasmid amplification. Plasmids were all derived from the original plasmid pSI1 containing nucleotides 1−4894 of the MoMuLV genome (1 being the first nucleotide of genomic RNA) under the control of the promoter of RNA polymerase from phage T7 (*41*). Cleavage by *Alu*I (position 210), *Hin*dIII (position 564), or *Bst*EII (position 725) provided DNA templates for RNAs A, AB, or ABC, respectively. Plasmids pBC and pC were produced by subcloning PCR fragments into the *Eco*RI−*Bam*HI sites of pUC18. The 5′ oligonucleotide primers contained an *Eco*RI restriction site, the T7 promoter, and viral sequences allowing transcription starting at positions 218 (PB5′) and 564, respectively (PC5′). The 3′ oligonucleotide primer (PC3′) corresponded to positions 704−731 of MoMuLV and contained a *Bam*HI site. Templates for transcription of RNA B (218−564) and RNA BC (218−725) were obtained by cleavage of pBC with *Hin*dIII and *Bst*EII, respectively. Cleavage of pC with *Bst*EII yielded the template for RNA C (564−725). DNA B was also directly obtained by PCR amplification from pSI1, using PB5′ and an oligonucleotide (PB3′) containing sequence 548−564 of MoMuLV. These constructions allowed synthesis of RNAs devoid of nonviral sequences. After PCR, DNA fragments were purified on low-melting agarose gel, and DNA was extracted by phenol/chloroform and precipitated with ethanol prior to T7 transcription.

Plasmids carrying single deletions ($pAB_{H2H3}C$, $pAB_{H1H3}C$, and $pAB_{H1H2}C$) and a triple deletion ($pAB_{\Delta 3H}C$) were obtained by a two-step PCR method using pSI1 as a template (*42*). Plasmids containing double deletions ($pAB_{H1}C$, $pAB_{H2}C$, and $pAB_{H3}C$) were constructed by inverse PCR on pSI1 derivative plasmids containing single mutations. The corresponding DNA templates were obtained either by linearization with *Bst*EII (DNA ABC) or PCR amplification using PB5′ and PB3′ as primers (DNA B).

DNAs obtained from linearized plasmid or PCR amplification were transcribed with phage T7 RNA polymerase as previously described (*23*). Following DNAse treatment, RNAs were extracted with phenol/chloroform and precipitated twice with ethanol. RNAs were then purified by spinning on small Sephadex G50 columns in MilliQ water. The purity and integrity of the synthesized RNAs were controlled by polyacrylamide gel electrophoresis under denaturing conditions. The RNA concentration was measured by UV absorbance at 260 nm. Internally labeled RNAs were synthesized using [α-^{32}P]ATP (Amersham) during transcription (37.5 μM [α-^{32}P]ATP/50 μCi/μg of the DNA template). RNAs were purified by polyacrylamide gel electrophoresis under denaturing conditions, eluted, and desalted on Sephadex G50.

In Vitro RNA Dimerization and Derived Procedures. RNA dimerization was conducted according to the standard procedure described in ref *23*. RNAs in MilliQ water at the appropriate concentration were heated at 90 °C for 2 min and chilled on ice for 2 min. After addition of a 5-fold dimerization buffer [final concentrations of 50 mM sodium cacodylate (pH 7.5), 300 mM KCl, and 5 mM $MgCl_2$], samples were incubated at 50 °C for 30 min and chilled on ice. Monomer controls were obtained by incubating RNAs after the denaturation step in monomer buffer [final concentrations of 50 mM sodium cacodylate (pH 7.5), 40 mM KCl, and 5 mM $MgCl_2$] at 20 °C for 30 min. Samples were analyzed on 1.2% agarose gels at 4 °C. Electrophoresis buffer and gels contained 45 mM Tris borate (pH 8.3) and 0.1 mM $MgCl_2$.

For the determination of the apparent dissociation constant (K_d), the RNA concentration was varied between 0.1 nM and 2.5 μM and a constant amount of labeled RNA (1000 cpm), corresponding to a negligible concentration of RNA (<10 pM), was added. Dimerization was conducted under standard dimerization conditions (see above). Gels were fixed with 10% trichloroacetic acid and dried, and the radioactivity was quantified on a BAS 2000 bioimager (Fuji). Quantification was assisted by either the Fuji or whole band analyzer (Bio Image) software. The K_d was determined as described previously (*31*). The fraction of RNA dimer $f_D^{(w/w)}$ was defined as the weight-to-weight ratio of the dimer to the total RNA species. All experiments were conducted at least twice. A difference of K_d was estimated to be significant when exceeding a factor of 4−5-fold. As already observed (*31*), different estimations of the background radioactivity by the different softwares accounted for the high variability of the K_d determinations. Particular adaptations of the dimerization protocol (competition, association, and dissociation kinetics experiments) are described in the Results.

RESULTS

Possible Existence of Multiple and Independent Dimerization Sites. Although the DLS is thought to be located in the Ψ domain, probing experiments showed that dimerization-induced reactivity changes were also found in regions upstream and downstream of Ψ, which were mostly interpreted as the result of conformational changes (*24*). The three hairpins, H1−H3, located in Ψ were thought to represent putative dimerization elements. Only the involvement of H1 appeared to be well-established (*25*, *26*). Nevertheless, it was suggested that sequences in the 3′ part of Ψ (364−565) could stabilize the dimer (*26*). However, most previous studies had been conducted on truncated RNA fragments and not in a larger, more natural context. Here, we addressed the following questions. (i) Are dimerization signals restricted to the Ψ domain? (ii) Do structural elements of Ψ other than H1 participate to the dimerization process? (iii) If several elements are involved, what are their relative contributions to the process?

To answer these questions, we constructed a series of truncated mutants corresponding to the structural domains defined in RNA nucleotides 1−725 (Figure 2): the Ψ domain (RNA nucleotides 218−564, named B), the upstream domain (RNA nucleotides 1−210, named A), and the downstream domain (RNA nucleotides 564−725, named C), as well as the various combinations of these domains, AB (RNA nucleotides 1−564), BC (RNA nucleotides 218−725), and the full fragment ABC (RNA nucleotides 1−725). We also constructed a series of mutants in the B and ABC contexts, containing combinations of single, double, and triple deletions of stem−loop motifs H1 (positions 278−303), H2 (positions 310−352), and H3 (positions 355−374) (Figure 2). For convenience, the resulting RNA mutants will be referred to by the stem−loop structures still present (i.e. the deletion of H1 in the ABC or B context will be named ABC_{H2H3} and B_{H2H3}, respectively). Otherwise, RNAs without

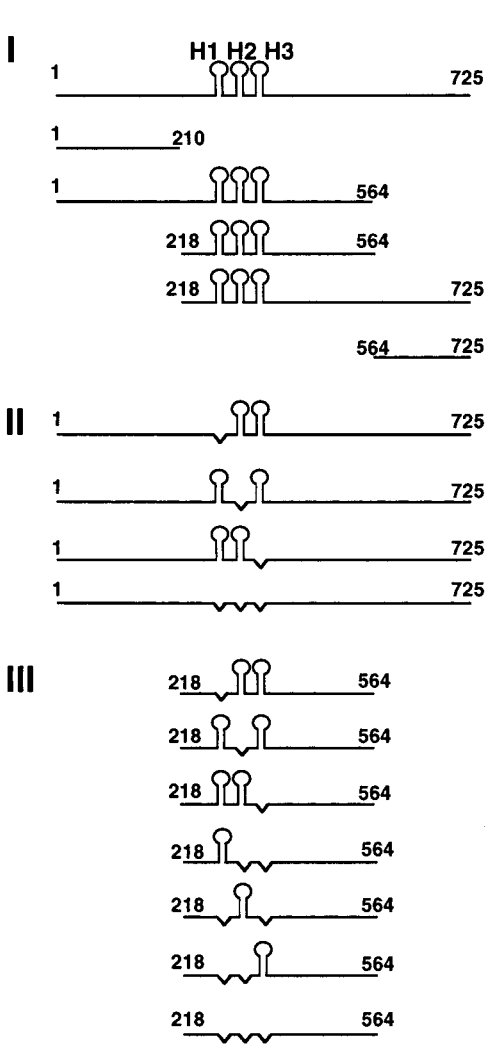

RNA	Kd (nM)	% dimerization
ABC	40	80
A	700	55
AB	20	95
B	40	80
BC	8	80
C	0.7	60
ABC_{H2H3}	40	80
ABC_{H1H3}	35	90
ABC_{H1H2}	70	60
$ABC_{\Delta 3H}$	250	60
B_{H2H3}	25	60
B_{H1H3}	5	85
B_{H1H2}	40	85
B_{H1}	5	65
B_{H2}	220	30
B_{H3}	50	65
$B_{\Delta 3H}$	$> 10^4$	< 5

FIGURE 2: Schematic representation of the different RNA mutants synthesized and their apparent K_ds. H1−H3 are shown by schematic stem−loop structures: (I) wild-type truncated fragments, (II) deletion fragments in the ABC context, and (III) deletion fragments in the B context. The percentage of dimerization observed at the plateau is indicated (with ±5% as a standard error).

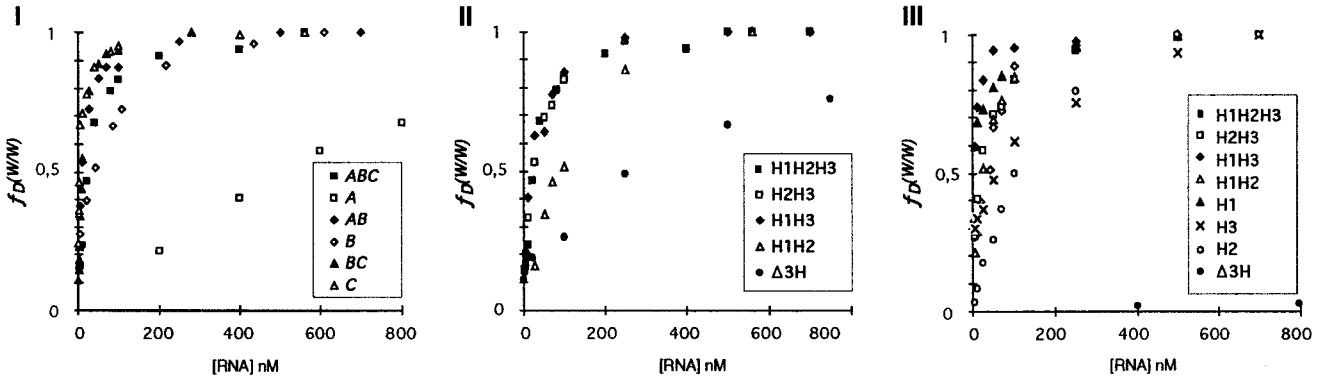

FIGURE 3: Effect of the various deletions on RNA dimerization. Fraction of RNA dimers $f_D^{(w/w)}$ as a function of RNA concentration. The saturation curves are grouped according to Figure 2, and the symbols are indicated in the insets. For a better comparison of K_ds, the value of $f_D^{(w/w)}$ at the plateau was normalized to 1. The percentage of dimerization at the plateau is indicated in Figure 2.

deletions will be referred as ABC and B, and RNAs containing the simultaneous deletion of the three motifs will be referred as $ABC_{\Delta 3H}$ and $B_{\Delta 3H}$. All RNAs were tested for dimerization under standard conditions, and dimerization efficiency was estimated by their apparent dissociation constants (K_d). Saturation curves are shown in Figure 3, and results are summarized in Figure 2. The percentage of dimerization at the plateau was found to vary. A decreased yield of dimerization at saturation was assumed to reflect a lower portion of the given RNA monomers being competent for dimerization or/and a weaker stability of the dimer which dissociates during electrophoresis.

RNAs ABC and B dimerize with the same efficiency (K_d = 40 nM), in agreement with previous observations that the dimers formed with these two fragments melt at the same temperature (*41*). RNA A shows some dimerization proper-

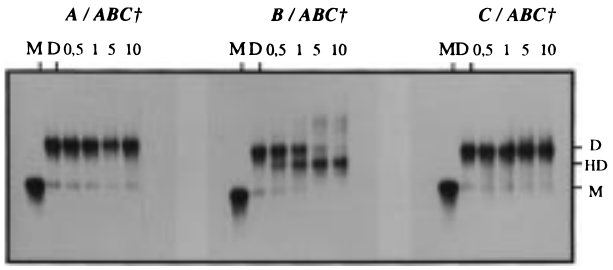

FIGURE 4: Competition experiments between RNA ABC and RNAs A−C. Labeled RNA ABC (denoted with a †) at a constant concentration of 200 nM was allowed to dimerize in the presence of unlabeled RNAs A−C added at the indicated molar excess (0.5−10-fold). The monomeric (M), dimeric (D), and heterodimeric (HD) forms were fractionated by agarose gel electrophoresis. The gel was fixed and autoradiographed.

ties, but with a very low efficiency (K_d = 700 nM), while RNA C dimerizes with a higher efficiency than RNA ABC itself (K_d = 0.7 nM). On the other hand, RNA AB dimerizes with a K_d similar to that of RNA ABC or B (20 nM) and RNA BC shows a K_d value between those of RNAs B and C (8 nM), but closer to that from RNA B than that from RNA C. Therefore, each subdomain (A−C) appears to display intrinsic dimerization properties but dimerizes with a markedly different efficiency. However, the dimerization of isolated domains A and C is clearly modulated by their context.

Dimerization Is Driven by Domain B. The previous results indicated that several elements are able to promote dimerization, depending on the context and experimental conditions. However, it is important to discriminate between the elements which specifically govern dimerization and those that might take place under particular circumstances. Since measuring K_d does not allow discrimination between specific and spurious elements, we tested the ability of truncated fragments to compete with RNA ABC for dimerization. The premise of these experiments is that an RNA starting at position 1 and spanning the first 725 nucleotides would probably be more representative of the in vivo process than shorter truncated fragments. In these experiments, labeled RNA ABC (200 nM) was allowed to dimerize in the presence of increasing amounts of unlabeled RNA A, B, or C (100 nM to 2 μM). The concentrations were chosen to allow a complete dimerization of RNA ABC and possible competition with the short RNA fragments. A clear inhibition of the formation of the RNA ABC homodimer is observed when RNA B is used as a competitor (Figure 4). In this case, an intermediate band corresponding to a heterodimer between RNAs ABC and B appears at a 0.5:1 B:ABC molar ratio. Equal amounts of homo- and heterodimers are observed at a 1:1 ratio, and at higher concentrations, RNA B is able to totally displace RNA ABC. Similar behaviors are observed when RNAs AB and BC are used as competitors (results not shown). On the other hand, neither RNA A nor RNA C is able to compete with RNA ABC, although they can homodimerize at the concentrations used in the assay. These experiments clearly demonstrate that the dimerization of RNAs ABC and B is specifically triggered by common elements. Note that the deletion of the three H1−H3 hairpins in RNA B abolishes dimerization (Figure 2). Thus, the low level of dimerization of RNA $AB_{\Delta 3H}C$ can probably be attributed to domains A and C. Indeed, RNAs A and C are able to form heterodimers with RNA $AB_{\Delta 3H}C$, while RNA B or ABC cannot (results not shown). Taken together, these observations indicate that the specificity of dimerization is provided by domain B (most likely involving hairpins H1−H3) and not by domain A or C, or by other parts of domain B.

H1−H3 Participate in the Dimerization Process. Unexpectedly, the deletion of H1, although identified as the essential element of dimerization, does not markedly affect the K_d, in either the ABC or B context (Figure 2). However, it was previously reported that RNA nucleotides 215−565 depleted of the 3′ part of H1 (nucleotides 290−299) does not significantly dimerize at low ionic strength and in the absence of Mg^{2+} (*25*). We verified that RNA B_{H2H3} does not form dimers under such conditions (results not shown). Furthermore, an oligonucleotide complementary to nucleotides 275−291 was able to inhibit dimerization of RNA nucleotides 215−565 at low ionic strength (100 mM NaCl) but not at high ionic strength (250 mM NaCl) (*26*). Otherwise, deletion of either H2 or H3 in both the B and ABC contexts does not markedly affect dimerization. Among the double deletions tested in the B context, only the simultaneous deletion of H1 and H3 significantly increases the K_d with a significant decrease of the dimerization yield at the plateau (Figure 2). It is noteworthy that a strong inhibition of dimerization in RNA ABC is only attained by the simultaneous deletion of H1−H3. The same deletion results in a complete inhibition of dimerization in the B context under the conditions tested. It was verified by chemical probing experiments that the conformation of the remaining part of B is not altered by the deletion of H1−H3 (results not shown). Thus, the loss of dimerization can be directly correlated to the absence of these three stem−loop strcutures and not to a more general change in secondary structure. Hence, these results suggest that the dimerization process is more complex than expected and probably involves several elements, displaying distinct roles or/and functional redundancy.

Relative Contributions of Stem−Loop Structures H1−H3 in the Dimerization Process. To specify the relative contributions of H1−H3, we performed a combinatorial analysis of the ability of the various possible deletion mutants (each able to form homodimers) to form heterodimers with other RNAs. To detect the formation of heterodimers, we used RNAs of different lengths (RNAs ABC and B). In these experiments, a constant amount of labeled RNA in the ABC context (200 nM) was dimerized in the presence of increasing amounts of unlabeled competitor RNA in the B context (200 nM and 1 and 2 μM). The resulting labeled products (ABC monomer and dimer and ABC−B heterolength dimer) were fractionated on agarose gels, and the radioactivity was quantified (see examples in Figure 5). Since all the tested RNAs are able to form homodimers, a competition between homo- and heterodimerization is expected. This will be revealed by the ability of RNAs to form heterodimers at a 1:1 molar ratio, and the effect will be further amplified when one of the two RNAs is added in excess. Only RNAs sharing identical or equivalent dimerization elements will exhibit identical behavior no matter which of the two RNAs is added in excess

The different RNA couples can be arranged according to their ability to form heterodimers (Table 1). Three groups

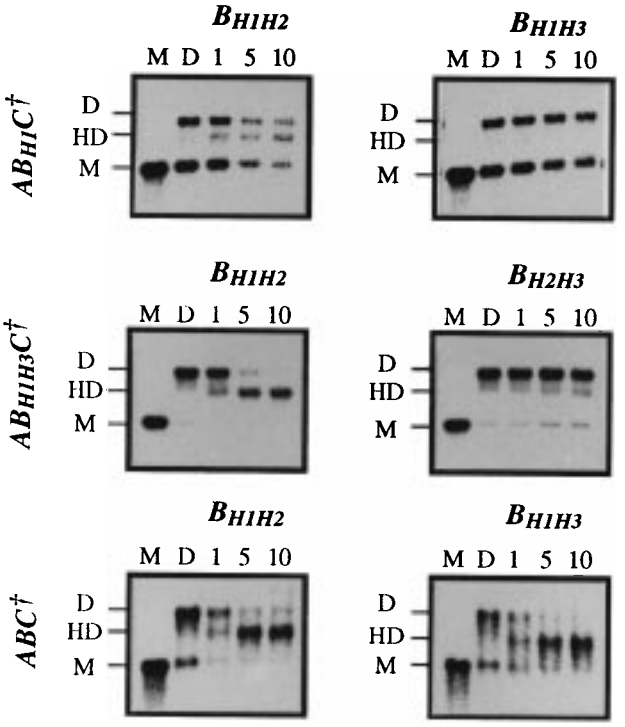

FIGURE 5: Competition experiments between various combinations of hairpin deletion mutants. The legend is the same as that used in Figure 4. The labeled RNA (200 nM) is indicated on the right side, and the unlabeled competitor is indicated above each autoradiogram.

can be defined according to their capacity to form either none or a low or high yield of heterodimers. As expected, the yield of heterodimerization was found to vary depending on which one of the two partners is added in excess. This distribution can be partially correlated to the presence or the absence of H1 in both RNAs. Indeed, none of the RNAs that do not share H1 are able to form heterodimers at a 1:1 molar ratio; most of them do not form heterodimers even in the presence of a 10-fold molar excess of the competitor RNA (Table 1), suggesting that H1 is absolutely required for heterodimerization. A few of RNAs exhibit weak dimerization when an excess of the B-type RNA is added. All these RNAs share H3 ($AB_{H1H3}C-B_{H3}$, $ABC-B_{H2H3}$, $AB_{H2H3}C-B_{H3}$, and $B_{H3}-AB_{H2H3}C$). Reciprocity is observed only in the case of the H2H3−H3 combination.

On the other hand, most of the RNAs that share H1 are able to form heterodimers even at a 1:1 molar ratio (8 of the 12 tested combinations) (Table 1). Nevertheless, the presence of H1 in both RNAs is not sufficient to ensure heterodimerization. Indeed, none of the RNAs exhibiting combinations H1H2H3−H1 and H1H3−H1 are able to form heterodimers at a 1:1 molar ratio and yield only very low amounts of heterodimer when H1 is added in excess. Thus, the presence of H3 (regardless of the presence of H2), in addition to H1, strongly favors the formation of homodimers versus heterodimers. On the other hand, the two H1−H1H2 combinations both promote significant amounts of heterodimerization, but increased homodimerization is observed when RNA containing H1H2 is added in excess over RNA containing H1 alone (Figure 5). Thus, H2 is also able to favor homodimerization in combination with H1, but to a lesser extent than H3. In agreement with this conclusion, both H1H3 and H1H2 efficiently form heterodimers with H1H2H3, with a minor advantage in the case of H1H3 when added at a 1:1 ratio (Figure 5). These observations underscore the fact that H1 and H3 are the optimal combination triggering dimerization and suggest that H2 can be recruited in absence of H3.

Table 1: Heterodimerization Properties of the Various Combinations of Deletion Mutants Involving Hairpins H1−H3[a]

	RNA combinations		*B*/*ABC*† molar ratio			
	B context	*ABC*† context	1x	5x	10x	
no H1 as a common element	*H3	H1H2H3	-	-	-	none
	*H2	H1H2H3	nd	nd	nd	
	*H3	H1H2	-	-	-	
	*H1	H2H3	-	-	-	
	*H2	H2H3	-	-	-	
	*H2	H1H3	nd	nd	nd	
	*H2H3	H1H2	-	-	-	
	H1H3	H2H3	-	-	-	weak or none
	H2H3	H1H3	-	±	±	
	H1H3	H3	-	-	-	
	H3	H1H3	-	±	±	
	H1H2H3	H2H3	-	-	-	
	H2H3	H1H2H3	-	±	+	
	*H3	H2H3	-	±	±	
H1 as a common element	H1H2H3	H1	-	-	-	
	H1	H1H2H3	-	±	±	
	H1H3	H1	-	-	-	
	H1	H1H3	-	±	±	
	*H1H3	H1H2H3	+	++	++	high
	H1H2H3	H1H2	±	+	++	
	H1H2	H1H2H3	±	++	++	
	H1H2	H1	±	+	+	
	H1	H1H2	±	++	++	
	H1H3	H1H2	±	+	+	
	H1H2	H1H3	±	++	++	

[a] Labeled RNA ABC† (200 nM) was allowed to dimerize in the presence of unlabeled RNAs A−C added at the indicated B/Abc† molar excess (0.5−10-fold). Hairpin elements present in each RNA context are indicated. The two reciprocal combinations for a given mutation couple are linked by a hyphen. An asterisk (*) indicates that the same results are obtained in the two reciprocal contexts. The results are expressed as follows: (−) 0−5%, (±) 5−30%, (+) 30−60%, and (++) 60−100% of the radioactivity in the heterodimer band (HD) compared to that of the ABC-type RNA homodimer.

Association and Dissociation Kinetics of the RNA Dimers. To define more precisely the functional role of each element in the dimerization mechanism, we compared the association and dissociation kinetics of wild-type RNA B with the kinetics of different RNA mutants containing either one single element (B_{H1}, B_{H2}, and B_{H3}) or two elements (B_{H1H2} and B_{H1H3}). RNAs were uniformly labeled with ^{32}P, and dimer formation was allowed under standard conditions, using identical concentrations of RNA (500 nM), with the exception of RNA B_{H2} (1 μM). These concentrations were chosen to allow optimal dimerization for each mutant. Aliquots were analyzed by gel electrophoresis after different incubation times. Results are shown in Figure 6A. Dimerization of RNA B is a fast event, as 50% of the dimer can be obtained after a 1 min incubation time. Unexpectedly, the dimerization of RNA B_{H1} is markedly slower, since 50% of the dimer is attained only after incubation for 6−7 min. However, the presence of H3 or H2 alone is able to confer a fast association (even slightly higher in the case of H3), close to that of the wild-type combination (Figure 6A). Moreover, the addition of H3 to H1 restores a wild-type

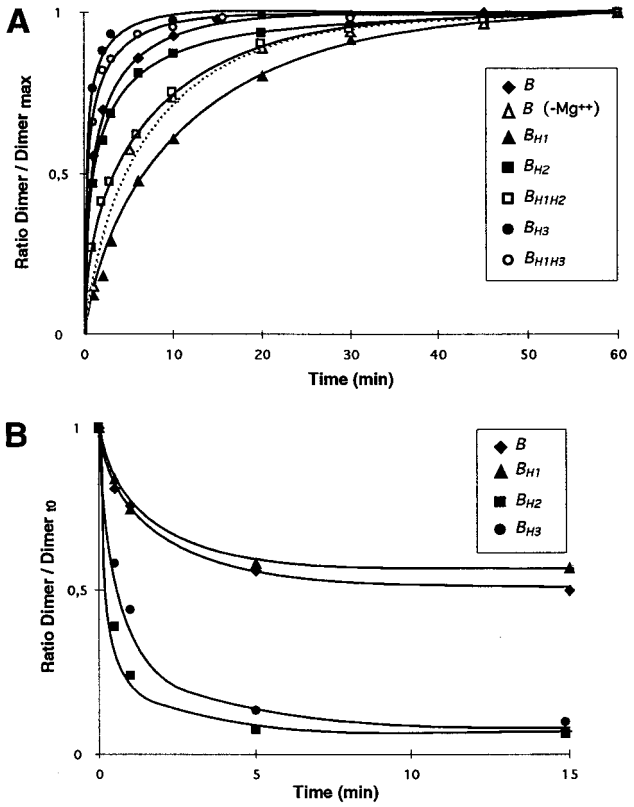

FIGURE 6: Kinetics of dimerization of various RNA B mutants. (A) Kinetics of association of the various RNAs. Labeled RNAs (500 nM, except for B_{H2} which was at 1 μM) were allowed to dimerize under standard conditions. Aliquots were taken at timed intervals, mixed with loading buffer, and loaded on native agarose gels. Dimerization and gel analysis of RNA B (without Mg^{2+}) were carried out under the same conditions, except that Mg^{2+} was omitted in dimerization and migration buffers. Results are expressed as the weight-to-weight ratio of the dimers formed at a given time to the maximum level of dimers formed at the plateau. (B) Kinetics of dissociation of the RNA dimers. Labeled RNAs were allowed to dimerize for 45 min under standard conditions. One microliter of the reaction mixture was diluted in a large volume (500 μL to 1 mL) of dimerization buffer. Aliquots were taken and analyzed as above. Results are expressed as the weight-to-weight ratio of remaining dimer to dimer formed at time 0 of dissociation. Symbols are indicated in the insets.

association rate. The addition of H2 also causes an increased association rate, but to a lesser extent than the addition of H3 (Figure 6A). Therefore, both H3 and H2 appear to act as kinetics enhancers, with H3 > H2. A similar effect was observed when dimer association was measured at 37 °C (data not shown), indicating that the kinetic effect of H3 and H2 is independent of temperature reaction. In addition, the kinetic effect exerted by H3−H2 is dependent on the presence of Mg^{2+}. Indeed, dimerization of RNA B is reduced in the absence of Mg^{2+} (Figure 6A). This might parallel the fact that RNA B_{H2H3} requires Mg^{2+} to dimerize (see above).

In dissociation experiments, RNAs were first dimerized as above for 45 min. Dissociation was then achieved by 500−1000-fold dilution with dimerization buffer at 50 °C. Final concentrations were below the measured K_d values (at least 10-fold). It was further verified that no detectable dimer was formed under these conditions. Aliquots were taken at various time intervals and analyzed by gel electrophoresis. In these experiments, it appears that dimers formed with either RNA B_{H2} or B_{H3} are rapidly dissociated (half-dissociation in less than 1 min) (Figure 6B). On the contrary, only a fraction (~40%) of the dimers formed with both RNA B and RNA B_{H1} dissociate rapidly (Figure 6B). The rest does not dissociate, even after several hours (results not shown). The same results were obtained when preformed dimers were diluted with water at 4 °C, instead of dimerization buffer. The existence of two populations with different stabilities is still not understood. One might postulate that the dissociable portion of the dimer is either partially or not correctly folded.

Nevertheless, H1 on one side and H3−H2 on the other side play distinct roles in the dimerization process. H1 is required to trigger a stable interaction. However, this interaction, which is a slow process, is kinetically enhanced by H3 and to a lesser extent by H2. Accordingly, RNAs B, B_{H1}, and B_{H1H3} yielded similar sharp melting temperature profiles (T_m = 60 °C; results not shown), confirming that H1 governs dimer stability. However, RNAs B_{H3} and B_{H2} did not display a discrete melting temperature typical of standard RNA dimers. This is most likely due to fast reassociation of the dimer when loading on the analysis gel. Complete dissociation could only be observed at high temperatures, corresponding to the secondary structure melting of the monomeric form.

DISCUSSION

Specificity of Dimerization. Although an autocomplementary sequence forming a stem−loop structure (H1) located in the Ψ domain (here named B) has previously been shown to be involved in the formation of the MoMuLV RNA dimer, several ambiguities still persisted about the possible implication of other RNA regions (*24*, *26*). Here, we systematically reinvestigate the dimerization properties of the first 725 nucleotides of the MoMuLV RNA and identify the specific elements that direct RNA dimerization. First, we show that truncated RNAs corresponding to both upstream (domain A) and downstream (domain C) regions of domain B are able to dimerize with different efficiencies. However, the elements responsible for the dimerization of the isolated A and C fragments are not involved in the dimerization of the larger ABC fragment (nucleotides 1−725), since they are both unable to interfere with the dimerization of RNA ABC. On the other hand, the fact that RNA B dimerizes with the same K_d as RNA ABC, and is indistinguishable from RNA ABC in competition assays, indicates that the dimerization of large RNAs is specifically driven by domain B. The most likely explanation is that isolated domains A and C adopt particular conformations that do not form in a larger context. This is probably correlated with the conformational versatility observed for these two domains depending on renaturation conditions, as well as different possibilities of interactions between the two domains (*24*). Unlike domains A and C, the isolated domain B behaves like RNA ABC, consistent with previous observations that it adopts the same structure independent of its context (*23*). RNAs B and ABC most likely represent good models of genomic RNA dimerization since the conformation of the dimer formed in vitro with these RNAs (*23*) was found to be very similar to that of the genomic RNA inside the virion (*43*).

The observation that dimers formed of truncated RNAs exhibit properties different from the properties of those

obtained with larger fragments is not unique. Indeed, a truncated fragment from HaSV was reported to melt at a lower temperature than a larger fragment or viral RNA (*38*). On the other hand, a truncated fragment from HIV-1, lacking sequences upstream of the SD site (containing the DIS), was shown to melt at a temperature higher than that of RNAs starting at position 1 or viral RNA (*35*). In ASLV, a short fragment from the 5′ end was reported to form dimers but not heterodimers with larger RNA (*44*). These examples are not exhaustive, since most studies on RNA dimerization have been conducted so far on truncated fragments. Hence, it is essential to carefully monitor the context effects on dimerization. Determination of the melting temperature or K_d alone is not sufficient, and further investigations are required.

Different Elements with Distinct Roles Are Important for Efficient Dimerization. Having determined the specific involvement of H1−H3 in domain B in driving dimerization, we investigated the specific roles of these elements in this process. Using competition experiments for the formation of homodimer molecules, we confirm that the palindromic stem−loop H1 is essential for triggering specific dimerization, but our results show that H1 alone does not ensure optimal dimerization. The optimal combination appears to be H1H3(±H2), and H2 is able to partially replace H3. We investigated the role of H1−H3 more precisely by kinetic experiments. We showed that dimers involving only the H1 interaction have a markedly reduced association rate as compared to the wild-type RNA B and that the addition of H3 is able to increase the association rate to the wild-type level. H2 is also able to enhance the dimerization rate, but to a lesser extent. On the other hand, interactions promoted by H3 or H2 alone are highly dynamic (rapid association and dissociation kinetics). Our results shed new light on the dimerization process that substantially differs from that previously proposed. According to the present data, the initial recognition, allowing a rapid and dynamic association, is ensured by H3 and to lesser extent by H2, while stabilization of the dimer requires the palindromic H1 element.

Initiation of dimerization was initially postulated to be promoted by a loop−loop interaction involving the palindromic H1 loop (UAGCUA), most likely followed by extension of intermolecular annealing (*25*, *26*). Here, we have shown that dimerization promoted by H1 alone or in the absence of Mg^{2+} and salt is a slow process, in agreement with previous observation of Girard et al. (*25*, *26*). We have also shown that most of the dimers formed with H1 alone do not dissociate within hours (as the wild-type RNA B). Loop−loop interactions are known to be dynamic and dissociate within seconds to minutes, while extended duplexes have much slower dissociation rates (*45*, *46*). However, we failed to detect a transient reversible duplex even after short incubation times (in the minute range), whenever dimers were formed at 37 or 50 °C (results not shown). A possible explanation is that the conversion from the loop−loop interaction to the extended duplex is extremely rapid. It is also known that the H1 region shows structural heterogeneity in the RNA monomer (*23*) and that only a fraction of the monomers folds into a conformation suitable for the loop−loop recognition. Accordingly, increasing the temperature of incubation is found to increase the dimerization yield, most likely by increasing the fraction of RNA conformers that are able to dimerize (*25*, *26*). This conformational rearrangement probably represents the rate-limiting step of the reaction and is responsible for the slow association rate observed for H1 alone. Therefore, our data indicate that H1-mediated dimerization probably involves extended intermolecular interactions through stem−loop opening, as proposed by Girard et al. (*25*, *26*). However, the transient loop−loop interaction does not appear to be responsible for the initial recognition event. Otherwise, the fact that a portion of dimers involving H1 (±H3 and H2) is still able to dissociate might reflect a structural defect of the RNA monomers resulting in an incorrect H1−H1 interaction.

The next question to be addressed concerns the mechanism by which H3 (or H2) enhances the dimerization rate. The H3 motif is a highly structured hairpin with a G•C rich stem (up to six G•C pairs out of a total of eight base pairs). The stem is closed by a GACG tetraloop, which adopts a highly organized structure, as shown by its lack of reactivity to chemical reagents in both monomer and dimer forms (*23*). Moreover, the tetraloop of H3 is followed on the 3′ side by UC, resulting in a six-base palindromic sequence (GACGUC). Interestingly, stem−loop H2 which can be recruited as a kinetic enhancer in the absence of H3 (but with a lower efficiency) contains the same GACG tetraloop. However, contrary to the H3 tetraloop, the H2 tetraloop is not part of a palindromic sequence. This observation argues against a standard loop−loop model if we assume that H3 and H2 can be alternatively used through a similar mechanism. An alternative mechanism might be envisioned if we consider that the GACG loop represents an essential recognition motif that might be recognized by an unknown receptor. This might be reminiscent of the recognition of GNRA tetraloops by specific receptors (*47*, *48*). Our previous results pointed to the role of Mg^{2+} in inducing a proper conformation of the GACG loop (*23*). This parallels the observation that dimerization of RNA B depleted of H1 requires high salt concentrations and/or the presence of Mg^{2+} (this study) (*25*). Accordingly, the kinetics of dimerization of wild-type RNA B is decreased in the absence of Mg^{2+} (Figure 6B). Thus, the kinetic effect of H3 and H2 is most likely governed by the proper conformation of the GACG loop mediated by Mg^{2+}. Our data are thus consistent with the observations showing that nucleotides 364−565 could increase the kinetics of dimerization in a salt-dependent manner (*26*). However, according to our data, this effect was most likely due to the fact that the RNA used (nucleotides 215−365) lacked the 3′ half of stem−loop H3 (and therefore the GACG loop) and not due to the absence of sequences located downstream of H3. Moreover, we found that RNA $B_{\Delta 3H}$ does not dimerize, although it contains all the sequences postulated to form intermolecular interactions.

In conclusion, while confirming the essential role of H1 in the dimerization mechanism, our results lead to a complete redefinition of it. Furthermore, we identify a novel element that plays a major role in this process. Fast recognition between the two monomers is facilitated by H3, most likely through the conserved GACG loop, and the resulting fast dissociating complex is then converted into a stable complex by H1 interaction. Direct recognition by H1 is also possible, but probably does not use a loop−loop intermediate as shown by slow association and dissociation rates. Therefore, H3

acts as a kinetic enhancer. Strikingly, the H2 element which also contains a GACG loop is able to play the same role as H3, although with a diminished efficiency. In particular, it can be recruited in absence of H3. It is not clear whether this functionally redundant element is also used in the presence of H3. Otherwise, the exact role of NCp in this process and any further maturation events (*49*, *50*) also remains to be understood. Remarkably, motifs H2 and H3 are both required for the encapsidation of MoMuLV RNA (*16*), and analogous motifs both containing a GACG tetraloop are also necessary for efficient RNA packaging in SNV (*39*). The single deletion of one of these two motifs only partially affects encapsidation in both systems. In addition, remarkable similarities are found between requirements for MoMuLV RNA encapsidation and dimerization. Indeed, the deletion of H1 reduces MoMuLV RNA encapsidation by 4−8-fold, and the complete loss of encapsidation is only attained upon deletion of the three motifs, H1−H3 (*16*, *22*). In HIV-1, mutations or deletions of the DIS motif have also been shown to reduce the encapsidation level (*15*, *17*, *18*). Therefore, these results reinforce the idea that RNA dimerization and packaging are closely related processes during the course of virion assembly.

ACKNOWLEDGMENT

We are grateful to F. Winter for skilful technical assistance. We acknowledge J. C. Paillart, R. Marquet, and J. S. Lodmell for fruitful discussions. R. Marquet and J. S. Lodmell are thanked for critical reading of the manuscript.

REFERENCES

1. Bender, W., Chien, Y. H., Chattopadkyay, S., Vogt, P. K., Gardner, M. B., and Davidson, N. (1978) *J. Virol. 25*, 888−896.
2. Kung, H. G., Hu, S., Bender, W., Bailey, J. M., Davidson, N., Nicolson, M. O., and McAllistair, R. M. (1976) *Cell 7*, 609−620.
3. Coffin, J. (1984) in *RNA Tumor Viruses* (Weiss, R., Teich, N., Varmus, H., and Coffin, J., Eds.) Vol. 1, pp 261−368, Cold Spring Harbor Laboratory Press, Cold Spring Harbor, NY.
4. Hu, W. S., and Temin, H. M. (1990) *Proc. Natl. Acad. Sci. U.S.A. 87*, 411−419.
5. Hu, W. S., and Temin, H. M. (1990) *Science 20*, 1227−1233.
6. Temin, H. M. (1991) *Trends Genet. 7*, 71−74.
7. Panganiban, A. T., and Fiore, D. (1990) *Science 241*, 1064−1069.
8. Jones, J. S., Allan, R. W., and Temin, H. M. (1993) *J. Virol. 67*, 3151−3158.
9. Bieth, E., Gabus, C., and Darlix, J.-L. (1990) *Nucleic Acids Res. 18*, 119−127.
10. Darlix, J.-L., Gabus, C., Nugeyre, M. T., Clavel, F., and Barré-Sinoussi, F. (1990) *J. Mol. Biol. 216*, 689−699.
11. Prats, A. C., Roy, C., Wang, P., Erard, M., Housset, V., Gabus, C., Paoletti, C. L., and Darlix, J.-L. (1990) *J. Virol. 64*, 774−783.
12. Katoh, I., Yasunaga, T., and Yoshinaka, Y. (1993) *J. Virol. 67*, 1830−1839.
13. Torent, C., Gabus, C., and Darlix, J.-L. (1994) *J. Virol. 68*, 661−667.
14. Paillart, J.-C., Marquet, R., Skripkin, E., Ehresmann, C., and Ehresmann, B. (1996) *Biochimie 78*, 639−653.
15. McBride, S. M., and Panganigan, A. T. (1996) *J. Virol. 70*, 2963−2973.
16. Mougel, M., Zhang, Y., and Barklis, E. (1996) *J. Virol. 70*, 5043−5050.
17. Paillart, J.-C., Berthoux, L., Ottmann, M., Darlix, J.-L., Marquet, R., Ehresmann, B., and Ehresmann, C. (1996) *J. Virol. 70*, 8348−8354.
18. Berkhout, B., and van Wamel, J. L. B. (1996) *J. Virol. 70*, 6723−6732.
19. Gorelick, R. J., Nigada, S. M., Arthur, L. O., Henderson, L. E., and Rein, A. (1991) in *Advances in molecular biology and targeted treatment of AIDS* (Kumar, A., Ed.) pp 257−272, Plenum Press, New York.
20. Mann, R., Mulligan, R. C., and Baltimore, D. (1983) *Cell 33*, 153−159.
21. Mann, R., and Baltimore, D. (1985) *J. Virol. 54*, 401−407.
22. Mougel, M., and Barklis, E. (1997) *J. Virol. 71*, 8061−8065.
23. Tounekti, N., Mougel, M., Roy, C., Marquet, R., Darlix, J.-L., Paoletti, C., Ehresmann, B., and Ehresmann, C. (1992) *J. Mol. Biol. 223*, 205−220.
24. Mougel, M., Tounekti, N., Darlix, J.-L., Paoletti, J., Ehresmann, B., and Ehresmann, C. (1993) *Nucleic Acids Res. 21*, 4677−4684.
25. Girard, P.-M., Bonnet-Mathonière, B., Muriaux, D., and Paoletti, J. (1995) *Biochemistry 34*, 9785−9794.
26. Girard, P.-M., de Rocquigny, H., Roques, B.-P., and Paoletti, J. (1996) *Biochemistry 35*, 8705−8714.
27. Skripkin, E., Paillart, J.-C., Marquet, R., Ehresmann, B., and Ehresmann, C. (1994) *Proc. Natl. Acad. Sci. U.S.A. 91*, 4945−4949.
28. Skripkin, E., Paillart, J.-C., Marquet, R., Blumenfeld, M., Ehresmann, B., and Ehresmann, C. (1996) *J. Biol. Chem. 271*, 28812−28817.
29. Laughrea, M., and Jetté, L. (1994) *Biochemistry 33*, 13464−13474.
30. Paillart, J.-C., Marquet, R., Skripkin, E., Ehresmann, B., and Ehresmann, C. (1994) *J. Biol. Chem. 269*, 27486−27493.
31. Paillart, J.-C., Skripkin, E., Ehresmann, B., Ehresmann, C., and Marquet, R. (1996) *Proc. Natl. Acad. Sci. U.S.A. 93*, 5572−5577.
32. Clever, J. L., Wong, M. E., and Parslow, T. G. (1996) *J. Virol. 70*, 5902−5908.
33. Muriaux, D., Girard, P.-M., Bonnet-Mathonières, B., and Paoletti, J. (1995) *J. Biol. Chem. 270*, 8209−8216.
34. Muriaux, D., Fossé, P., and Paoletti, J. (1996) *Biochemistry 35*, 5075−5082.
35. Marquet, R., Paillart, J.-C., Skripkin, E., Ehresmann, C., and Ehresmann, B. (1994) *Nucleic Acids Res. 22*, 145−151.
36. Laughrea, M., and Jetté, L. (1996) *Biochemistry 35*, 1589−1598.
37. Laughrea, M., and Jetté, L. (1996) *Biochemistry 35*, 9366−9374.
38. Feng, Y.-X., Fu, W., Winter, A. J., Levin, J. G., and Rein, A. (1995) *J. Virol. 69*, 2486−2490.
39. Yang, Y., and Temin, H. M. (1994) *EMBO J. 13*, 713−726.
40. Sambrook, J., Fritsch, E. F., and Maniatis, T. (1989) in *Molecular cloning. A laboratory manual*, Cold Spring Harbor Laboratory Press, Cold Spring Harbor, NY.
41. Roy, C., Tounekti, N., Mougel, M., Darlix, L., Paoletti, C., Ehresmann, C., and Ehresmann, B. (1990) *Nucleic Acids Res. 18*, 7287−7292.
42. Landt, O., Grunert, H.-P., and Hahn, U. (1990) *Gene 96*, 125−128.
43. Alford, R. L., Honda, S., Lawrence, C. B., and Belmont, J. W. (1991) *Virology 183*, 611−619.
44. Fossé, P., Motté, N., Roumier, A., Gabus, C., Muriaux, D., Darlix, J.-L., and Paoletti, J. (1996) *Biochemistry 35*, 16601−16609.
45. Eguchi, Y., and Tomizawa, J. (1990) *Cell 60*, 199−209.
46. Eguchi, Y., and Tomizawa, J. (1991) *J. Mol. Biol. 220*, 831−842.
47. Costa, M., and Michel, F. (1995) *EMBO J. 14*, 1276−1285.
48. Costa, M., and Michel, F. (1997) *EMBO J. 16*, 3289−3302.
49. Fu, W., Gorelick, R. J., and Rein, A. (1994) *J. Virol. 68*, 5013−5018.
50. Fu, W., and Rein, A. (1993) *J. Virol. 67*, 5443−5449.

BI9800303